

A Hydrodynamic Theory for Cavitating Delta Wing Hydrofoils

PAUL KAPLAN,* THEODORE R. GOODMAN,† AND C. C. CHEN‡
Oceanics Inc., Plainview, N. Y.

The status of available hydrodynamic theories of cavitating flow past delta wing hydrofoils is reviewed, and it is found that asymptotic results for limiting conditions of cavitation (i.e., large and small cavitation numbers) in earlier work by Tulin are incorrect. The mathematical problem of conical flow for cavitated delta wings of fairly wide apex angles is recast with a new "closure" condition replacing the previous condition of no source-like flow in a transverse plane. The results obtained for lift coefficient, for apex angles up to 60° , as a function of angle of attack and cavitation number, are compared with available experimental data. The comparison indicates good agreement of the new theory for delta wings with apex angles up to 45° . Examination and comparisons of the slender-body theory of Cumberbatch and Wu shows the limits of applicability of that theory to be restricted to large angles of attack ($>17^\circ$) and small apex angles ($<15^\circ$). Thus, differences in results obtained using different mathematical and physical models are delineated, together with information on the respective regions of validity.

Nomenclature

A	= coefficient in cavity area representation
A_i	= coefficients of the complex potential expansion
a	= nondimensional magnitude of the transverse velocity on the cavity
C_L	= lift coefficient
c	= $(1 - \lambda^2)^{1/2}$
$E(k)$	= complete elliptic integral of the second kind
$f(x)$	= potential due to thickness
$g(x)$	= term in expression of cross-flow potential
h	= cavity thickness measured from and normal to the wing surface
$K(k)$	= complete elliptic integral of the first kind
k	= modulus of the elliptic integrals
L	= lift
l	= nondimensional width of the cavity measured in the transverse plane from the leading edge to the in-board end of the cavity
n	= normal direction
p	= pressure
p_∞	= pressure at infinity
p_c	= pressure on the cavity
$S(x)$	= cavity area
$s(x)$	= local foil span
U	= velocity of the oncoming uniform stream
v	= vertical velocity
w	= transverse velocity
x, y, z	= coordinate system defined by Fig. 2
Z	= $\bar{z} + i\bar{y}$, transverse plane complex variable
α	= angle of attack
β	= apex angle
γ	= parameter of elliptic integral of the third kind
ζ	= $\xi + i\eta$, transformed plane complex variable
λ	= $1 - l$
ν	= $w - iw$, complex velocity in the transverse plane
$\Pi(\gamma^2, k)$	= complete elliptic integral of the third kind
ρ	= fluid density
σ	= cavitation number
Φ	= perturbation velocity potential
$\bar{\Phi}$	= complex potential in the transverse plane
ϕ	= two-dimensional perturbation potential in the transverse plane
$\bar{\phi}$	= nondimensional cross-flow potential

Introduction

THE development of hydrofoil craft is presently oriented toward high-speed operation, where cavitated flow occurs. This flow condition results from the reduced local pressures associated with the high speed, and/or ventilation from the atmosphere. For various situations of practical interest it appears that low-aspect-ratio hydrofoils will be used in such craft, especially because of their structural advantages. One particularly important class of low-aspect-ratio hydrofoil planforms is a delta wing, for which theoretical hydrodynamic studies have been carried out by Tulin¹ and by Cumberbatch and Wu.²

Both studies^{1,2} are based upon a slender-body-theory approach, but the physical model for cavity shape is different for each theory. Tulin's model assumes that the cavity covers only part of the foil, a region adjacent to each of the leading edges of the delta wing, with a wetted region between the inner termini near the wing centerline. The Cumberbatch and Wu model considers the cavity to envelop the entire upper surface of the wing and to close at some point downstream of the foil's trailing edge. The range of applicability of each theory and the degree of agreement with available experimental data were not known. Only limited numerical evaluations of the Cumberbatch-Wu theory were available (for small-apex-angle delta wings). No numerical results of any extent were available for the Tulin theory except for asymptotic results in two limiting cases, viz., for very large and for very small cavitation numbers.

Following publication of Refs. 1 and 2, two sets of experiments^{3,4} on cavitating delta wings were carried out. Reichardt and Sattler³ measured the forces acting on a series of delta wings with different apex angles, ranging from narrow to wide deltas. Kiceniuk⁴ measured the lift force on narrow delta wings. Both sets of investigators made visual observations of the flow and cavity characteristics, and from these it could be concluded that the Cumberbatch-Wu model was valid for very narrow delta wings at large angles of attack, whereas the Tulin model was applicable to wings with larger apex angles. No detailed comparison of the theoretically predicted forces with the experimental results was presented.

The first aim of this paper was to extend Tulin's work in order to determine the hydrodynamic forces for the complete range of cavitation numbers and apex angles. The second objective was to carry out further numerical evaluations of the Cumberbatch-Wu theory and then to compare the results of the two theories with the available experimental data.

Received May 16, 1967. Prepared for Office of Naval Research under Contract Nonr-4329(00), NR 062-230. [3.07]

* President. Member AIAA.

† Vice President. Associate Fellow AIAA.

‡ Staff Scientist; now at University of California, San Diego, La Jolla, Calif.

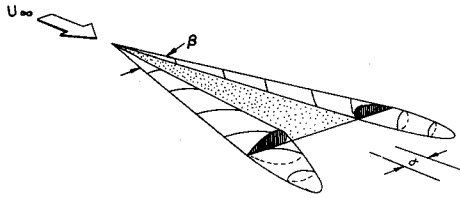


Fig. 1 Cavitation on a delta wing.

In pursuing the first objective it was discovered that the limiting values for lift calculated by Tulin did not follow from his theory. It was also discovered that the zero source strength condition that Tulin uses in developing his theory is inconsistent with his conical flow assumption. It was necessary, therefore, to recast the problem and resolve it completely before numerical results of any validity could be obtained, or any comparison with experiments could be made. This reworking of Tulin's model then became the primary purpose of this paper.

A cavity closure condition is proposed to replace Tulin's zero source strength condition. The requirement of no sourcelike flow in the transverse plane is inconsistent with the conical flow requirement, which specifies that all transverse coordinates vary linearly with x (the longitudinal coordinate), while cross-sectional areas vary as x^2 . Similarly, conical flow requires that the total velocity potential should be linear in x ; the original Tulin model does not satisfy this condition. The capability of the newly formulated model, with the cavity closure boundary condition, to satisfy these requirements will be demonstrated in the ensuing analysis.

The problem considered here is that of the cavity flow past a delta wing placed at a small angle of attack in an otherwise uniform flow. Starting from the apex of the delta, the flow forms a cavity on the top of the plate; the cavity grows as the cavitation number is decreased. It is shown that the conical flow model with two cavities which is assumed here is valid for apex angles $\beta > 10^\circ$. Naturally, the flow is more conical near the apex of the delta than near the trailing edge. The system of the wing and the cavity is assumed to be slender so that slender-body theory may be used. A potential flow model is assumed throughout the flowfield. The boundary condition that the flow must be tangential to the boundary is applied both on the cavity and on the wetted part of the wing. In addition, on the cavity the pressure must be constant. It is only necessary to solve the transverse problem in one transverse plane of the wing since the flow is assumed conical. The problem is thus reduced to a two-dimensional, boundary-value problem with mixed boundary conditions. For the sake of convenience in calculating the complex velocity, the problem is transformed to another plane where the proper solution can be found more readily. The transformation and solution provided by Tulin are still useful and will be used here. The lift on the delta wing may then be determined by integrating pressures.

Formulation of the Problem

Figure 1 is a schematic diagram of the cavitating flow past a slender delta wing placed at a small angle in a uniform stream. Geometric and flow parameters are defined more fully in Fig. 2. A conical flow model is chosen for this cavity flow. Tulin's method is used for the initial analysis; however, the proper boundary condition is added and the subsequent analysis is different.

Assuming that the pressure at infinity is zero, the linearized Bernoulli equation gives

$$p = -\rho U (\partial \Phi / \partial x) \quad (1)$$

where Φ is the perturbation velocity potential. From Eq. (1), $\partial \Phi / \partial x$ is constant on the cavity since the pressure there is constant. The delta wing length is chosen to be unity.

The kinematic boundary condition states that the flow must be tangential to the wing and the cavity. Along the bottom of the wing and on the wetted portion of the top of the wing, the linearized boundary condition is

$$\partial \Phi / \partial y = -U \alpha \quad (2)$$

where α is the angle of attack.

According to slender-body theory,⁵ the potential of a slender body placed at an angle of attack α to the uniform stream is

$$\Phi(x, y, z) = \phi(y, z; x) + f(x) \quad (3)$$

where $\phi_{yy} + \phi_{zz} = 0$ and

$$f(x) = -\frac{U}{4\pi} \frac{\partial}{\partial x} \int_0^\infty S'(x_1) \frac{x - x_1}{|x - x_1|} \ln 2|x - x_1| dx_1 \quad (4)$$

and $S(x)$ is the cross-sectional area of the cavity at section x . In order for the flow to be conical it is necessary that S be of the form $S = Ax^2$ over the wing, where A is a constant. (The form that S takes in the wake is discussed in Appendix A, Ref. 8.)

The first term in Eq. (3), $\phi(y, z; x)$ is the potential of the cross flow in the transverse plane, and $f(x)$ is the potential due to thickness. For small angles of attack, the cavity thickness will also be small, and the boundary condition may be applied at the projection of the wing and cavity on the horizontal plane, i.e., along the top and bottom of a symmetrical slit on the z axis. Hence, by virtue of Green's theorem, the cross-flow potential is

$$\phi(y, z; x) = \frac{1}{2\pi} \oint \left(\frac{\partial \phi}{\partial n} - \phi \frac{\partial}{\partial n} \right) \ln[(z - z')^2 + y^2]^{1/2} dz' \quad (5)$$

Using the following transformation suggested by conical flow

$$\bar{y} = 2y/s \quad \bar{z} = 2z/s$$

Equation (5) becomes

$$\phi(y, z; x) = \frac{s(x)}{4\pi} \ln \frac{s(x)}{2} \oint \frac{\partial \phi}{\partial n} d\bar{z} + \frac{s(x)}{2} \bar{\phi}(\bar{y}, \bar{z}) \quad (6)$$

The linearized boundary condition on the top of the cavity is

$$\frac{v}{U} \equiv \frac{1}{U} \frac{\partial \phi}{\partial n} \equiv \frac{1}{U} \frac{\partial \phi}{\partial y} = -\alpha + \frac{\partial h}{\partial x} \quad (7)$$

where h is the thickness of the cavity. Substituting Eq. (7) into (6) leads to

$$\phi(y, z; x) = g(x) + [s(x)/2] \bar{\phi}(\bar{y}, \bar{z}) \quad (8)$$

where

$$g(x) = \frac{U}{4\pi} s(x) \ln \frac{s(x)}{2} \oint \frac{\partial h}{\partial x}(\bar{z}) d\bar{z} \quad (9)$$

and $\bar{\phi}(\bar{y}, \bar{z})$ is a harmonic function.

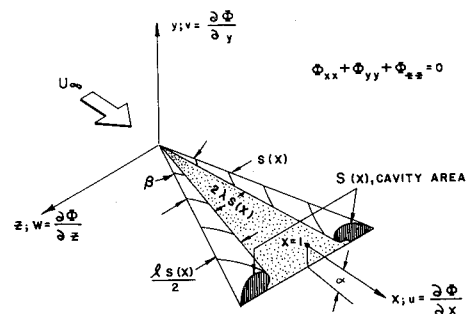


Fig. 2 Cavitating flow past a delta wing and the coordinate system.

Consider the pressure boundary condition on the cavity, $\lambda < |\bar{z}| < 1$. Upon substituting Eqs. (3) and (8) into (1), this condition becomes

$$\frac{\partial \Phi}{\partial x} = \frac{U}{2} \sigma = f'(x) + g'(x) + \frac{1}{2} \beta \left(\bar{\phi} - \bar{z} \frac{\partial \bar{\phi}}{\partial \bar{z}} \right) \quad (10)$$

where β is the apex angle ($s = \beta x$), $1 - \lambda$ is the nondimensional width of the cavity, and σ is the cavitation number, which is defined by

$$\sigma = (p_\infty - p_c) / \frac{1}{2} \rho U^2 \quad (11)$$

Now consider the boundary condition on the bottom of the wing and also on the wetted part of the top of the wing. Upon substituting Eqs. (3) and (8) into (2), this condition becomes

$$\partial \Phi / \partial y = -U\alpha = \partial \bar{\phi} / \partial \bar{y} \quad (12)$$

From Eq. (10) and the assumption of conical flow it follows that both $f'(x) + g'(x)$ and $[\bar{\phi} - \bar{z}(\partial \bar{\phi} / \partial \bar{z})]$ must be constant since $\partial \Phi / \partial x$ is constant on the cavity. It can be shown (see Appendixes, Ref. 8) that

$$f'(x) + g'(x) = (U/2\pi) A (\ln \beta - 3 \ln 2 + 3) \quad (13)$$

where

$$A = \frac{\beta}{2} \int_{-1}^1 \frac{\partial h}{\partial x} d\bar{z} = \frac{\beta}{2} \int_{-1}^1 \left(\frac{v}{U} + \alpha \right) d\bar{z} \quad (14)$$

Returning now to Eq. (10), this becomes a differential equation for $\bar{\phi}$ in terms of \bar{z} . Since $\bar{\phi}$ must be symmetric with respect to \bar{z} , the solution is

$$\bar{\phi}(0, \bar{z}) = (U/\beta) \sigma - (2/\beta) [f'(x) + g'(x)] - Ua|\bar{z}| \quad (15)$$

or

$$\begin{aligned} \partial \bar{\phi} / \partial \bar{z} &= -aU & \bar{z} > 0 \\ \partial \bar{\phi} / \partial \bar{z} &= aU & \bar{z} < 0 \end{aligned} \quad (16)$$

where aU is the unknown but constant magnitude of the transverse velocity on the cavity. There are now two unknown parameters in the problem, the transverse velocity which is measured by a and the width of the cavity which is measured by λ . In order to make the problem determinate it is necessary to specify two conditions. One condition is that the potential along the leading edge be specified. Upon substituting Eq. (13) into (15) and setting $\bar{z} = 1$, this condition becomes

$$\phi(0, 1) = U[(\sigma/\beta) - a] - (U/\pi\beta) A (\ln \beta + 3 - 3 \ln 2) \quad (17)$$

The second condition requires that the cavity surface be zero at the foil leading edges and also at the inboard ends; i.e., according to Fig. 3,

$$\begin{aligned} h(-\lambda, x) &= h(-1, x) = 0 \\ h(\lambda, x) &= h(1, x) = 0 \end{aligned} \quad (18)$$

From Eq. (7), we have

$$h = \int_{x_1}^x \left(\frac{v}{U} + \alpha \right) dx \quad (19)$$

where $x_1 = \pm 2z/\beta$ is a point on the leading edge (see Fig. 4).

Fig. 3 Closure conditions in transverse Z plane.

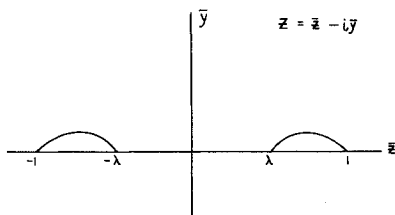
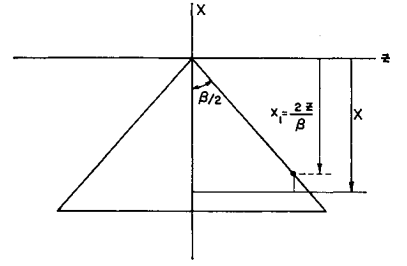


Fig. 4 Schematic diagram of the wing in xz plane.



With the definitions $\bar{z} = 2z/s$, $s = \beta x$, Eq. (19) becomes

$$h(\bar{z}, x) = -x\bar{z} \int_{\pm 1}^{\bar{z}} \left[\frac{v}{U} + \alpha \right] \frac{d\bar{z}}{\bar{z}^2} \quad (20)$$

As can be seen from Eq. (20) the conditions $h(\pm 1, x) = 0$ are satisfied identically. The two physical conditions used to calculate λ and a are Eq. (17) and

$$h(-\lambda, x) = x\lambda \int_{-1}^{-\lambda} \left[\frac{v}{U} + \alpha \right] \frac{d\bar{z}}{\bar{z}^2} = 0 \quad (21)$$

Now consider the lift on the delta wing. According to linear theory,

$$\frac{dL}{dx} = \int_{-s/2}^{s/2} [p(0-, z) - p(0+, z)] dz \quad (22)$$

Substituting Eq. (1) into (22), there results

$$\frac{dL}{dx} = -\rho U \int_{-s/2}^{s/2} \left[\frac{\partial \Phi}{\partial x}(0-, z) - \frac{\partial \Phi}{\partial x}(0+, z) \right] dz \quad (23)$$

and using both the conical transformation and the fact that ϕ is symmetric with respect to z , Eq. (23) becomes

$$\frac{dL}{dx} = -\rho U \frac{\partial}{\partial x} \frac{s^2(x)}{4} \int_{-1}^{+1} [\bar{\phi}(0-, \bar{z}) - \bar{\phi}(0+, \bar{z})] d\bar{z} \quad (24)$$

Thus,

$$L = -\rho U \frac{s^2(1)}{4} \int_{-1}^{+1} [\bar{\phi}(0-, \bar{z}) - \bar{\phi}(0+, \bar{z})] d\bar{z} \quad (25)$$

Introducing $\bar{\Phi} = \bar{\phi} - i\bar{y}$ as the complex potential in the transverse plane, Eq. (25) becomes

$$L = -\rho U \frac{s^2(1)}{4} \operatorname{Re} \oint \bar{\Phi} dZ \quad (26)$$

where the contour is taken along the real axis, $\bar{y} = 0$, and $Z = \bar{z} + i\bar{y}$. The potential $\bar{\Phi}$ can be expanded in a Laurent series, and takes the form

$$\bar{\Phi} = A_0 \ln Z + \frac{A_1}{Z} + \frac{A_2}{Z^2} + \dots \quad (27)$$

In general the A_n 's are complex. However it is shown in Ref. 6 that $A_0 = (U/2\pi)(dS/dx)$, a real quantity. Upon substituting Eq. (27) into (26), the lift becomes

$$\frac{L}{\frac{1}{2} \rho U s^2(1)} = -\operatorname{Re} [i\pi A_0 \bar{z}_0 + i\pi A_1] = -\operatorname{Re} (i\pi A_1) \quad (28)$$

The first term of this equation can be obtained by integrating by parts leading to $\oint \ln Z dZ = (Z \ln Z)_{\text{contour}} - \oint dZ$. The remaining contour integral vanishes identically and the integrated part becomes $2\pi i Z$, which, since $\bar{y} = 0$, reduces to $2\pi i \bar{z}$. Thus, since A_0 is real, the first term of Eq. (28) vanishes identically. Denoting $v = w - iw$ as the complex velocity in the transverse plane and $\tau = 1/Z$, Eq. (28) becomes, as also shown by Tulin,

$$\frac{L}{\frac{1}{2} \rho U s^2(1)} = \frac{\pi i}{2} \frac{d^2 v}{d\tau^2} \bigg|_{\tau=0} \quad (29)$$

cavity, is related to c as follows:

$$l = 1 - \lambda^2 = 1 - (1 - c^2)^{1/2} \simeq \frac{1}{2}c^2 \quad (\text{for } c \rightarrow 0) \quad (40)$$

and therefore Eq. (39) becomes

$$\frac{L}{\frac{1}{2}\rho U^2 s^2(1)} \doteq \frac{\pi\alpha}{2} \left(1 + \frac{1}{2}l\right) \quad (41)$$

Thus, even a small amount of cavitation will increase the lift above that found for the noncavitating case. Similar results occur in case of small partial cavitation in two-dimensional flow, which is ascribed to effective increase in camber due to cavity. This is also a possible explanation of the effect in the present situation.

For $c \rightarrow 1$, which represents a large cavity with both in-board edges coming together, we have

$$K(k) \rightarrow \infty \quad E(k) \rightarrow 1 \quad \Pi(\gamma^2, k) \rightarrow 2K(k)$$

and, therefore, Eq. (37) gives

$$a = [1/(2)^{1/2}K]\alpha\pi \quad (42)$$

Combining Eq. (42) with the asymptotic values of $K(k)$, $E(k)$, and $\Pi(\gamma^2, k)$ and substituting in Eq. (36), we obtain

$$\frac{L}{\frac{1}{2}\rho U^2 s^2(1)} \doteq \frac{\pi}{2} \alpha \left(\frac{1}{4} + \frac{1}{2K}\right) \doteq \frac{1}{8} \pi\alpha \quad (43)$$

Care must be taken in the derivation and use of the results of Eqs. (42) and (43), since we are working in the neighborhood where K is singular.

Equation (17) is used to find the expression for $\sigma/\alpha\beta$ in terms of c . In order to solve for $\sigma/\alpha\beta$, it is necessary to find the potential at $\bar{z} = 1$, $\bar{y} = 0$. The potential is defined as

$$\bar{\phi}(\bar{z}) - \bar{\phi}(\infty) = \int_{\infty}^{\bar{z}} w d\bar{z} \quad (44)$$

where the integral is taken along the real axis ($y = 0$) and with w the real part of the complex velocity v . By expanding Eq. (32) in terms of $(1/\zeta)$ for large ζ it is found that

$$\lim_{\zeta \rightarrow \infty} \nu(\zeta) = B \frac{1}{\eta} \quad (45)$$

where $B = -(2/\pi)(U/\beta)A$ and $\eta = \text{Im}(\zeta)$. Rewriting Eq. (44), we have

$$\int_{\infty}^{\bar{z}} \left\{ w(\bar{z}) - \frac{B}{\bar{z}} \right\} d\bar{z} = \bar{\phi}(\bar{z}) - B \ln \bar{z}$$

where the logarithmic infinity of the potential is cancelled by this method. Therefore

$$\bar{\phi}(1) = \int_{\infty}^1 \left\{ w(\bar{z}) - \frac{B}{\bar{z}} \right\} d\bar{z} \quad (46)$$

After evaluation, Eq. (46) becomes

$$\begin{aligned} \bar{\phi}(0,1) = & -2B \ln 2 + B \ln c + (2)^{1/2}B \ln[1 + (2)^{1/2}] + \\ & (U\alpha c/4) \{ 2 \ln[1 + (2)^{1/2}] - (2)^{1/2} \} + \\ & \frac{1}{(2)^{1/2}} \frac{U}{\pi} a \int_{x=1}^0 \int_{\xi_0=0}^c \left(\frac{x}{1+x} \right)^{1/2} \times \\ & \frac{\{ (c^2 - \xi_0^2)x - \xi_0^2 - c\xi_0 \}}{\xi_0^2 + (c^2 - \xi_0^2)x^2} F(\xi_0) dx d\xi_0 \quad (47) \end{aligned}$$

An exact evaluation of Eq. (47) requires numerical integration; however, the limiting values of $\sigma/\alpha\beta$ for $c \rightarrow 0$ and $c \rightarrow 1$ can be obtained. For the limit $c \rightarrow 0$, Eq. (47) becomes

$$\bar{\phi}(0,1) = [U/(2)^{1/2}]\alpha c D \quad (48)$$

where D is a bounded constant. Substituting Eq. (48) into (17), we have

$$\frac{U\alpha}{(2)^{1/2}} c D = U \left(\frac{\sigma}{\beta} - a \right) - \frac{U}{\beta} \frac{A}{\pi} (\ln \beta + 3 - 3 \ln 2) \quad (49)$$

and using the relation $\lim_{c \rightarrow 0} A = 0$ leads to

$$(\alpha c/2)D = (\sigma/\beta) - a \quad (50)$$

From Eq. (38), $a = 4\alpha/c$, and Eq. (50) then becomes

$$(\sigma/\alpha\beta) - (4/c) = [D/(2)^{1/2}]c$$

which becomes in the limit

$$\sigma/\alpha\beta \doteq 4/c \gg 1 \quad (51)$$

Examination of Eq. (38) results in the following expression for a , viz.,

$$a = \sigma/\beta \quad (52)$$

For the limiting condition where $c \rightarrow 1$, we have

$$\bar{\phi}(0,1) \doteq U\alpha(\ln 2 - \frac{1}{2}) + (U\alpha/2K)G \quad (53)$$

where G is a finite quantity, and thus (since $K \rightarrow \infty$)

$$\lim_{c \rightarrow 0} \bar{\phi}(0,1) \doteq U\alpha(\ln 2 - \frac{1}{2}) \quad (54)$$

Substituting this expression into Eq. (17) gives

$$U\alpha \left(\ln 2 - \frac{1}{2} \right) = U \left(\frac{\sigma}{\beta} - a \right) - \frac{UA}{\beta\pi} (\ln \beta + 3 - 3 \ln 2) \quad (55)$$

where $A = \frac{1}{4}\beta\alpha\pi$ and $a = (1/K)\alpha\pi$. Upon substitution, Eq. (55) reduces to

$$\sigma/\alpha\beta = \frac{1}{4}(1 + \ln 2 + \ln \beta) \quad (56)$$

where $\beta > 10^\circ$ so that the two-cavity flow model proposed here is applicable, because for $\beta < 10^\circ$, the quantity $\sigma/\alpha\beta < 0$, which is physically unreasonable. This restriction might also be explained as due to the requirement of a different cavity configuration for the case of narrow delta wings at low cavitation numbers, viz., the single cavity completely enveloping the wing upper surface, as proposed by Cumberbatch and Wu. Further discussion of this point will be given in the next section of the paper. To simplify the numerical calculation of Eq. (47), the double integral is integrated once with respect to the variable x to give a single integral, and then with $\xi_0 = c \cos \theta$ Eq. (47) becomes

$$\begin{aligned} \bar{\phi}(0,1) = & -2B \ln 2 + B \ln c - \frac{1}{2} U\alpha c + \\ & \frac{U\alpha c^2}{2(2)^{1/2}\pi} \int_{\pi/2}^0 \sin \theta \left(\frac{1 - \cos \theta}{1 - c^2 \cos^2 \theta} \right)^{1/2} \left\{ \ln R \left[-\cos \frac{\theta}{2} \cos \theta + \right. \right. \\ & \left. \left. \cot \theta \sin \frac{\theta}{2} (1 + \cos \theta) \right] - \left(\theta + \frac{\pi}{2} - \delta \right) \times \right. \\ & \left. \left[\frac{\cos \theta \sin \theta}{2} + \frac{\cos \theta}{2} \cot \theta (1 + \cos \theta) \right] \right\} d\theta \quad (57) \end{aligned}$$

where

$$\begin{aligned} R = & (1 + 4 \cos^2 \theta)^2 - 8 \cos^2 \theta + 4(2 \cos \theta)^{1/2} \sin(3\theta/2) + \\ & 8(2 \cos \theta)^{1/2} \cos \theta \cos \theta/2 \\ \delta = & \tan^{-1} \frac{3 \cos \theta + 2(2 \cos \theta)^{1/2} \cos \theta/2}{\sin \theta + 2(2 \cos \theta)^{1/2} \sin \theta/2} \end{aligned}$$

Equations (36, 37, and 57) are solved simultaneously to give numerical values of lift coefficient in terms of σ with α and β as parameters. The lift coefficient C_L in the present report is defined with the total wing area as the area reference, and thereby differs from the lift coefficient value defined by Tulin. However the definition used herein is the same as that used by Cumberbatch and Wu, as well as in both sets of experimental data, thereby facilitating comparisons between theory and experiment.

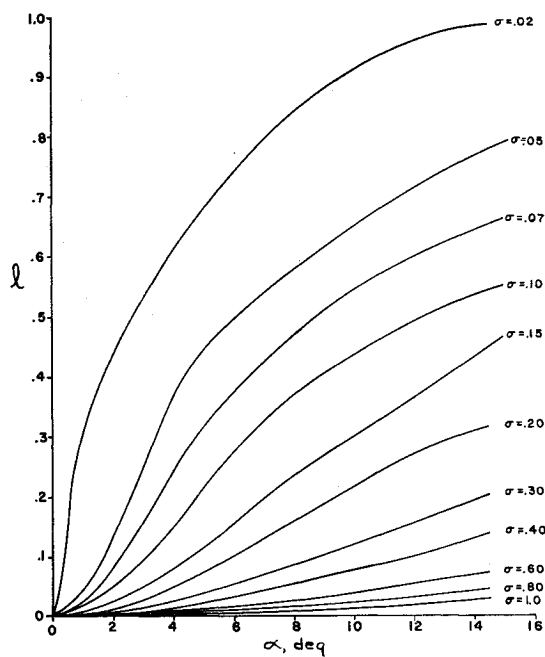


Fig. 7 Nondimensional width of the cavity vs angle of attack, $\beta = 15^\circ$.

Numerical Results and Discussion

In order to illustrate the range of validity of the present theory, as well as the theory developed by Cumberbatch and Wu,² comparisons will be made with the experimental data available in Refs. 3 and 4. The first numerical results presented herein are plots of the nondimensional cavity width parameter l vs angle of attack α , with cavitation index σ as a parameter. Figure 7 shows the results for a delta wing with $\beta = 15^\circ$, and Fig. 8 demonstrates the values for $\beta = 45^\circ$. Although no experimental values are given for comparison, comparing the results in these two figures yields information on the relative sizes of the cavities for the two different apex angles.

Curves of the lift coefficient C_L as a function of σ , for the various angles of attack tested in Ref. 3, are given in Figs.

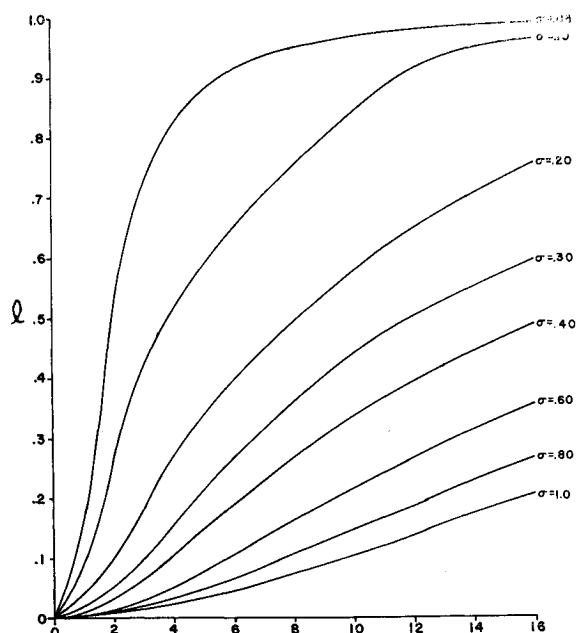


Fig. 8 Nondimensional width of the cavity vs angle of attack, $\beta = 45^\circ$.

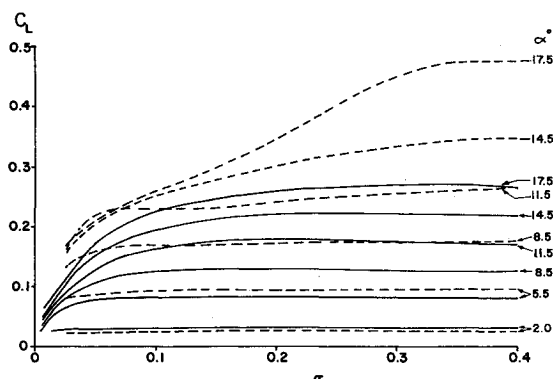


Fig. 9 Comparison of lift coefficient from present theory with experimental values in Ref. 3: $\beta = 15^\circ$, - - - experiment, — theory.

9–12 for four different delta wings, viz., $\beta = 15^\circ, 30^\circ, 45^\circ, 60^\circ$. The experimental values obtained in Ref. 3 are also plotted in these same figures, thereby allowing direct comparison between theory and experiment. Good agreement between the present theory and the experiments of Ref. 3 is exhibited for the configurations where $\beta = 30^\circ$ and 45° . For the case $\beta = 15^\circ$ good agreement is obtained only for $\alpha < 6^\circ$, and there is poor agreement for $\beta = 60^\circ$. For $\sigma < 0.10$ there is poor agreement for all the configurations regardless of the value of α or β . At the same time, the possibility of errors in the experimental data of Ref. 3 at such low cavitation numbers must be considered, especially in view of the nature of the freejet curvature in the water tunnel as well as the interference in the cavity pattern due to the sting support. Another comment as to the limitations of the theory concerns the case $\beta = 60^\circ$, where agreement should not be expected in view of the limits of applicability of slender-body theory to such a relatively wide wing, even for the case of noncavitating flow.

Similar plots are made for the values of C_L calculated from the Cumberbatch and Wu theory,² and these are presented in Figs. 13 and 14 for the configurations with $\beta = 15^\circ$ and 30° . Comparisons with the data of Ref. 3 were also made for the cases $\beta = 45^\circ$ and 60° , but the results are not shown in any of the figures. It is observed from all of these comparisons that there is hardly any agreement at all between the Cumberbatch-Wu theory and this set of experimental data, except for the case of the largest angle of attack ($\alpha > 17^\circ$) and then only for the case of the smallest apex angle configuration ($\beta = 15^\circ$).

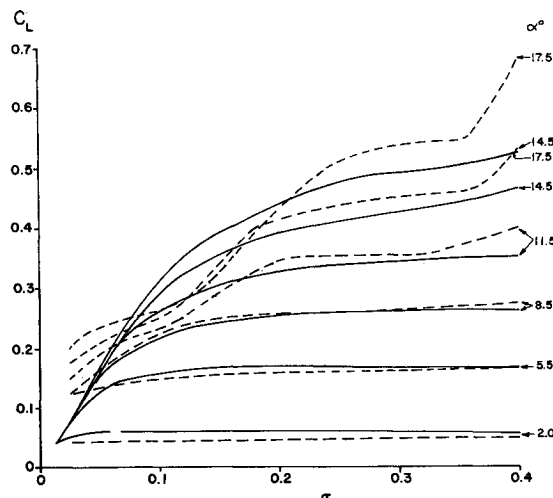


Fig. 10 Comparison of lift coefficient from present theory with experimental values in Ref. 3: $\beta = 30^\circ$, - - - experiment, — theory.

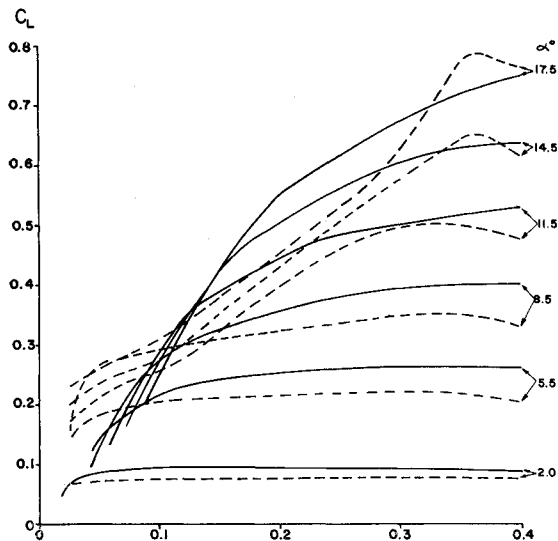


Fig. 11 Comparison of lift coefficient from present theory with experimental values in Ref. 3: $\beta = 45^\circ$, - - - experiment, — theory.

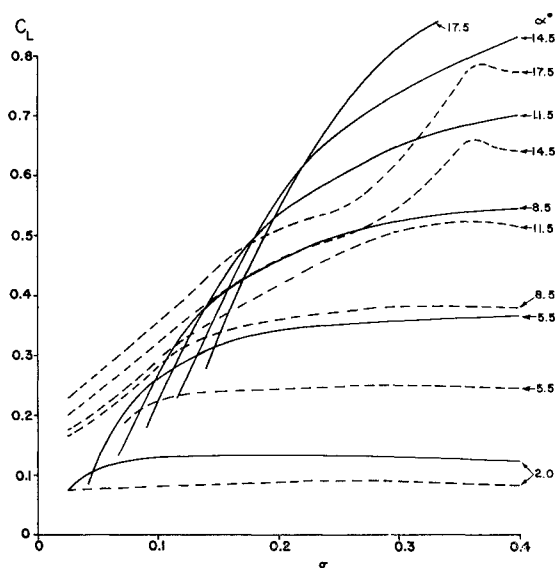


Fig. 12 Comparison of lift coefficient from present theory with experimental values in Ref. 3: $\beta = 60^\circ$, - - - experiment, — theory.

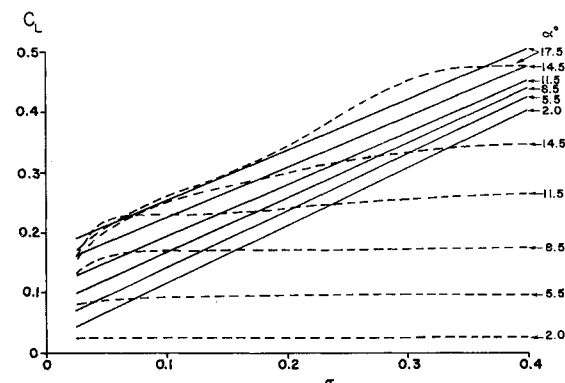


Fig. 13 Comparison of Cumberbatch-Wu theory with experimental values in Ref. 3: $\beta = 15^\circ$, - - - experiment, — theory.

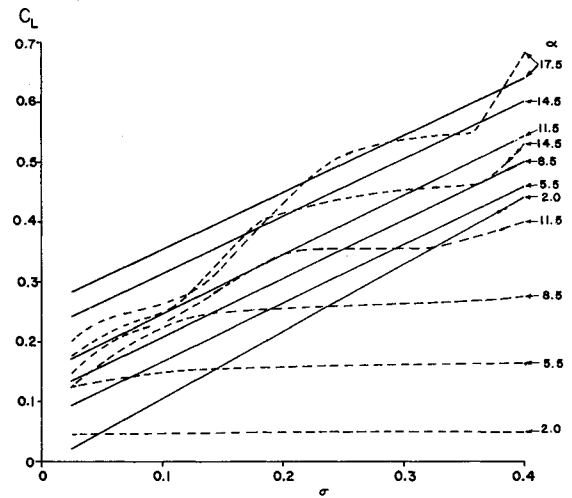


Fig. 14 Comparison of Cumberbatch-Wu theory with experimental values in Ref. 3: $\beta = 30^\circ$, - - - experiment, — theory.

In Figs. 15–17, values of C_L from the Cumberbatch-Wu theory are compared with data obtained in the California Institute of Technology water-tunnel tests,⁴ for delta wing configurations with $\beta = 10^\circ$, 15° , and 30° . The experimental data were measured at large angles of attack (ranging

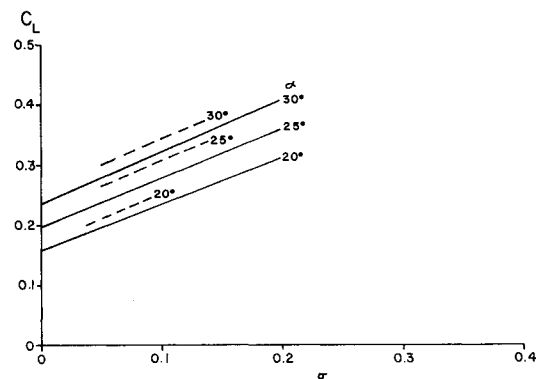


Fig. 15 Comparison of Cumberbatch-Wu theory with experimental values in Ref. 4: $\beta = 10^\circ$, - - - experiment, — theory.

from 10° to 30°) and also for relatively low cavitation numbers. It is found that there is fairly good agreement between the theory of Ref. 2 and this set of experiments for the smaller apex angles, $\beta = 10^\circ$ and 15° , while much poorer agreement is obtained for the wider delta wing, $\beta = 30^\circ$.

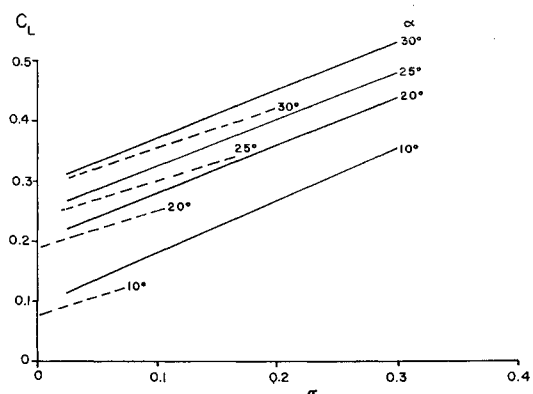


Fig. 16 Comparison of Cumberbatch-Wu theory with experimental values in Ref. 4: $\beta = 15^\circ$, - - - experiment, — theory.

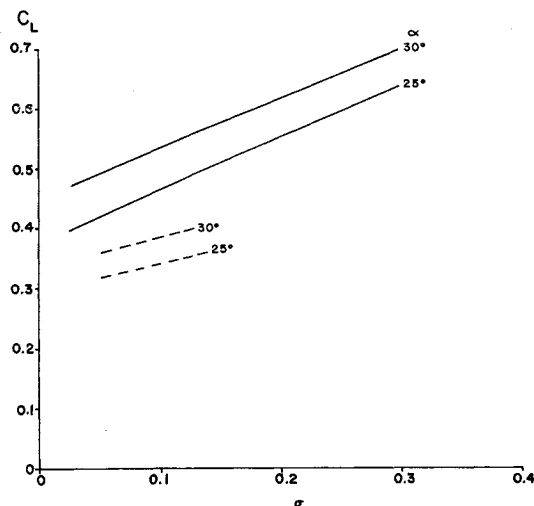


Fig. 17 Comparison of Cumberbatch-Wu theory with experimental values in Ref. 4: $\beta = 30^\circ$, - - - experiment, — theory.

The visual observations in Ref. 4 support the hypothesis of a large single cavity enveloping the foil upper surface for the case of large angles of attack, with small cavitation numbers, and also for narrow (small β) delta wing configurations. Similarly, the cavity observations and photographs presented in Ref. 3 support the two-cavity model originally proposed by Tulin and utilized in the present theoretical development for wider delta wings.

Although no extensive investigation has been carried out, the small effect of cavitation on the lift coefficient of a delta wing foil, for angles of attack up to 8° and cavitation numbers down to $\sigma = 0.18$ (as shown by the experiments in Ref. 3), indicates that lift performance close to noncavitating conditions can be achieved by such foils. Thus delta wing hydrofoil configurations can provide useful lift effects at speeds up to 70 knots while extensive cavitation is present, without any appreciable penalty due to that flow pattern.

Conclusions

On the basis of the numerical comparisons given previously, the conical flow model developed in this paper adequately describes the cavitating flow past delta wings, both qualitatively and quantitatively for moderate angles of attack (up to about 12°) and for apex angles up to about 45° . For smaller apex angles, e.g., $\beta = 15^\circ$, the valid angle-of-attack

range is up to 6° , while for $\beta = 30^\circ$ the angle-of-attack range extends up to about 17° as long as $\sigma > 0.10$. This particular theory is not necessarily restricted by linearity with regard to angle of attack, since nonlinear effects are present in the results, especially for the smaller cavitation numbers in the range of validity. This conclusion may be demonstrated more readily by plots of C_L vs angle of attack, with σ as a parameter, as shown in some of the graphs of experimental results in Ref. 3. Presentation of the theory in this manner has been checked, and the results support this conclusion.

The Cumberbatch-Wu theory² only appears to be valid for very narrow delta wings with large angles of attack and small cavitation numbers. These requirements are also necessary in order to obtain the large single cavity that is the physical model proposed in the analysis of Ref. 2.

The present investigation has delineated the regions of validity for the available hydrodynamic theories applicable to cavitating delta wing hydrofoils. Considering the practical application to a realistic hydrofoil craft, the theory developed within this paper is most appropriate to the wider delta wing configurations (β up to 45°) that would serve as support foils for high-speed vehicles. The possible small penalty in lift effectiveness due to cavitation for such foils, compared to the noncavitating foil performance, indicates the prospect of wider utility of such configurations in future hydrofoil craft development.

References

- ¹ Tulin, M. P., "Supercavitating flow past slender delta wings," *J. Ship Res.* **3**, 17-22 (December 1959).
- ² Cumberbatch, E. and Wu, T. Y., "Cavity flow past a slender pointed hydrofoil," *J. Fluid Mech.* **11**, 187-208 (1961).
- ³ Reichardt, H. and Sattler, W., "Three-component-measurements on delta wings with cavitation," Max-Planck-Institut für Strömungsforschung, Göttingen, Final Rept. (July 1962).
- ⁴ Kiceniuk, T., "Superventilated flow past delta wings," California Institute of Technology Rept. E-101.5 (July 1964).
- ⁵ Adams, M. C. and Sears, W. R., "Slender-body theory—review and extension," *J. Aerospace Sci.* **20**, 85-98 (February 1953).
- ⁶ Sacks, A. H., "Aerodynamic forces, moments, and stability derivatives for slender bodies of general cross section," NACA TN 3283 (November 1954).
- ⁷ Byrd, P. F. and Friedman, M. D., *Handbook of Elliptic Integrals for Engineers and Physicists* (Springer-Verlag, Göttingen, 1954).
- ⁸ Kaplan, P., Goodman, T. R., and Chen, C. C., "A hydrodynamic theory for cavitating delta wing hydrofoils," Oceanics Inc., Plainview, N. Y., TR67-33 (December 1966).